



High-bandwidth beam balance for vacuum-weight experiment and Newtonian noise subtraction

Enrico Calloni^{1,a} , Archimedes Collaboration², Virgo Collaboration³

¹ Università degli Studi di Napoli Federico II, Naples, Italy

² SAR-GRAV Laboratory, Sos Enattos, Lula, Nuoro, Italy

³ European Gravitational Observatory, Cascina, Pisa, Italy

Received: 19 November 2020 / Accepted: 9 February 2021

© The Author(s) 2021

Abstract We report the experimental results of a prototype balance for the Archimedes experiment, devoted to measure the interaction between quantum vacuum energy and gravity. The prototype is a *beam balance* working at room temperature which shares with the final balance several mechanical and optical components. The balance sensitivity has been tested at the site of the Virgo gravitational wave detector in order to benefit from its quiet environment and control facilities. This allowed also the test of the coherence of the balance data with the Virgo interferometer signal and with the environmental data. In the low-frequency regime, the balance has shown a sensitivity of about $8 \times 10^{-12} \text{Nm}/\sqrt{\text{Hz}}$, which is among the best in the world, and it is very promising toward the final Archimedes measurement. In the high-frequency region, above a few Hz, relying on the behavior of the balance as a rotational sensor, the ground tilt has been measured in view of the next work devoted to Newtonian noise subtraction (NNS) in Virgo. The measured ground tilt reaches a minimum of about $8 \times 10^{-11} \text{rad}/\sqrt{\text{Hz}}$ in the few Hz region and ranges from 10^{-10} to $10^{-9} \text{rad}/\sqrt{\text{Hz}}$ in the 10–20 Hz region, where a very interesting coherence, at some frequencies, with the Virgo interferometer signal is shown.

1 Introduction

In recent years, the measurement of small forces with macroscopic detectors has experienced an enormous development, driven by the interferometers for gravitational wave detection [1–7] and by the improvement of instruments like torsion pendulums and beam-balance rotational sensors [8–11]. Remarkably, torsion balances and rotational sensors, typically working in the mHz region, have shown a considerable overlap of interests both with space-based interferometers and with the ground-based gravitational wave detectors. In this latter case, the control loops, which keep the interferometers on their working point, can benefit, in the sub-Hz region, from a ground tilt signal provided by the rotational sensors [11, 12]. Furthermore, the sensitivity in the low-frequency range (around 10 Hz) of the ground-based detectors is expected to be limited by the so-called Newtonian noise in the next scientific runs [13, 14]. Rotational sensors will provide ground-motion signals useful to reconstruct the

^a e-mail: enrico.calloni@na.infn.it (corresponding author)

variation of the gravitational field and hence contribute to the subtraction of Newtonian noise from the gravitational wave signal [15].

Within the framework of macroscopic detectors of small forces, Archimedes collaboration recently proposed a beam balance to measure the force exerted by the gravitational field on a rigid Casimir cavity. The force to be measured is called the *Archimedes force of vacuum*, as it corresponds to the weight of the vacuum fluctuation modes that are expelled by the Casimir cavity [16, 17]. The measurement consists in detecting the weight variation of a layered type II superconductive sample around its transition [17]. The core of the apparatus will be a cryogenic balance whose design torque sensitivity is about $\tilde{\tau} = 6 \times 10^{-13} \text{Nm}/\sqrt{\text{Hz}}$ in the frequency range of tens of mHz or lower [18].

As described in this paper, the apparatus is a rotational sensor. Its characteristic features are low moment of inertia, low restoring force and low resonant frequency in order to maximize the sensitivity to the applied force [18]. To study the feasibility of such an extremely sensitive balance, a prototype working at room temperature has been built. To warrant high sensitivity, the balance readout is an interferometric system. Moreover, the final apparatus will work in a cryogenic environment that implies a long recovery time for each intervention on the balance. For this reason, the readout of the prototype balance has already been designed to be particularly robust and to have a high dynamic range, in order to pledge its capability in recovering the correct interferometer signal even in case of high deviations from the working point. The balance has been initially assembled and tested in the Naples laboratory; then, it has been installed at the Virgo site, which is seismically more quiet, specifically in the North-end building. In this setup, the balance has been tested for the torque sensitivity in the low-frequency regime, while at high frequencies it has been operated as a tiltmeter (rotational sensor). The results of these tests suggest that the balance is presently limited at low frequencies by actuator and sensing noises, while at high frequencies the balance is enough sensitive to measure the ground tilts and can be used for Newtonian noise subtraction. Interestingly, the balance signal is coherent, at some frequencies, with the output of the Virgo interferometer. Although this coherence is not due to Newtonian noise coupling of the ground tilt, it would help in identifying particular noise sources like, for example, diffused light from vibrating elements excited by ground motion.

The paper is organized as follows: In Sect. 2, the mechanical and optical schemes of the prototype balance are described. In Sect. 3, its low-frequency behavior is shown, and a discussion on the reached sensitivity and its possible increase is presented. In Sect. 4, the high-frequency behavior is illustrated, in particular, the use of the balance as a tiltmeter. Finally, the next steps toward further improvements for the balance performance is outlined in Sect. 5.

2 The balance prototype

The working prototype of Archimedes is a short-arm version of the final balance, with no samples suspended from its ends. Its core consists of a 50-cm-long arm, attached at its center through two thin wirelike suspensions (Fig. 1), in a configuration similar to LIGO rotation sensor [11]. Unlike this latter, however, the balance requires a high torque-to-tilt transfer function, which implies that momentum of inertia as well as suspension restoring force has to be as low as possible. To fulfill these specifications, the suspended arm is hollow and made of aluminum, leading to a momentum 0.013kg m^2 in the case of the prototype. In the final design of the balance, instead, the momentum is 0.72kg m^2 , since the arm length is 1.4 m and superconducting samples are suspended from its ends. The restoring force is kept low

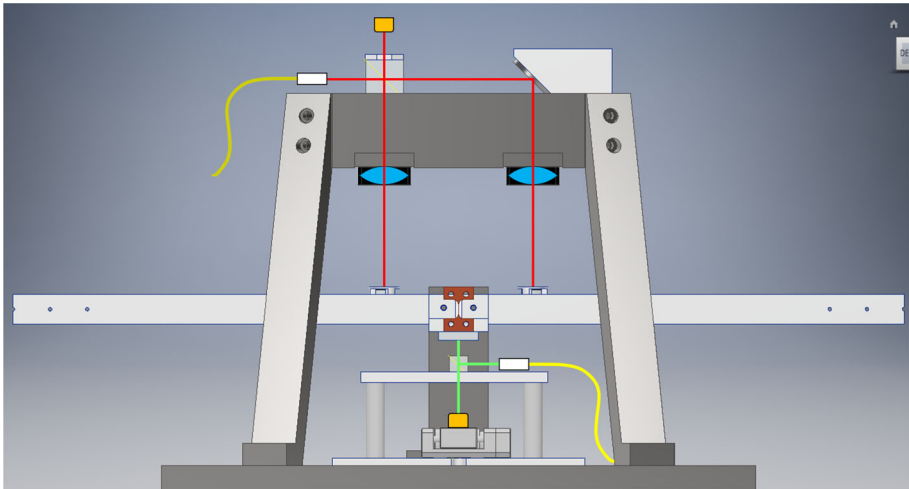


Fig. 1 Scheme of the balance prototype including the optical readout. Notice the two lenses (in light blue), with focal length equal to their distance from the arm. The displacement and relative tilts of the two beams recombining at the beam splitter are of the second order with respect to the arm tilt

by using thin suspensions with a $0.5\text{ mm} \times 0.1\text{ mm}$ section. This force, together with the distance between the arm center of mass and its center of rotation, determines the resonance frequency of the balance. The center of mass of the prototype has been tuned to be within $10\text{ }\mu\text{m}$ from the center of rotation, giving a resonance frequency of 25 mHz.

2.1 Optical readout: interferometer and optical lever

The balance angular motion can be monitored by two different optical readouts: a Michelson interferometer, with higher sensitivity, and an auxiliary optical lever, with wider dynamic range. Both the optical systems are physically bolted to the ground; hence, the arm angular motion is measured with respect to it. The interferometer has been designed with the following requirements: (1) minimize coupling with undesired degrees of freedom; (2) maintain good contrast even for relatively high tilts; and (3) allow realignment by moving optical elements not lying on the reference nor on the measurement arm.

The first condition has been obtained with the beams impinging on the mirrors perpendicularly. To keep a simple optical scheme, a Michelson interferometer with unequal arm lengths has been chosen, for a path length difference of 10 cm. In the present version of the prototype, the length difference is not compensated and the laser frequency is not yet stabilized. However, the frequency noise is not a limiting source in the present condition. Optical path compensation and laser frequency stabilization are planned for the next improvement of the balance.

The second condition has been fulfilled by designing the interferometer in such a way that the angular and translation separations of the two interfering beams are of the second order with respect to the arm tilts. This has been obtained by adding in both the beam paths a lens with focal length L_f equal to the distance between the lens itself and the mirror, so that the beam is focused on the arm mirror (see Fig. 1). This scheme allows also the fulfillment of the third specification. Indeed, if the arm tilt α is higher than a few mrad, the interferometer can be realigned by translating the input beam vertically by the quantity $\delta y = L_f \alpha$. In this

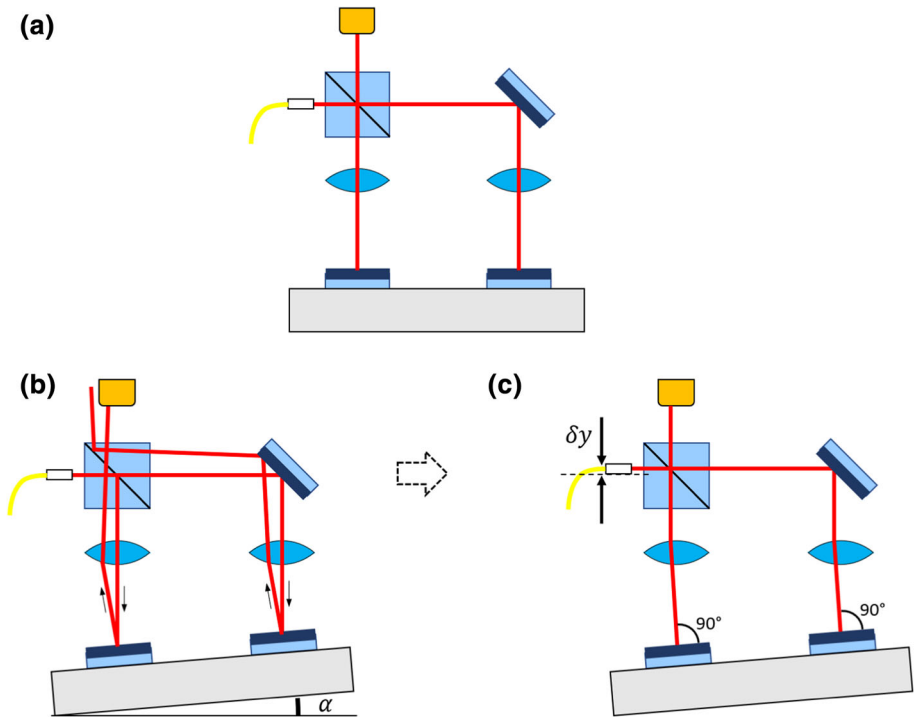


Fig. 2 Optical scheme of the interferometric readout. In figure (a), the interferometer is aligned, while the balance arm is horizontal. An arm tilt α would misalign the interferometer (b), but the presence of lenses in both arms permits the realignment by moving vertically the input laser beam by an amount δy (c)

condition, the beams impinge again orthogonally on the arm mirrors; then, they are reflected on the incoming path and recombine correctly at the beam splitter, as sketched in Fig. 2.

As mentioned above, the readout is completed by an auxiliary optical lever, powered by a superluminescent diode (SLED) and read by a quadrant photodiode. The lever is designed to have the beam impinging perpendicularly on a mirror placed on the lower face of the balance arm, and it is used as an initial reference position for the arm tilt.

2.2 Center of mass positioning

Beam balances and tiltmeter signals should not be induced by translation ground motion, but only by weight variations or ground rotations, respectively. It is known [19,20] that, if the tiltmeter center of mass does not lie on its rotation axis, a ground acceleration along the arm direction \vec{z} generates a torque on the arm $\tau = m\delta\ddot{z}$, where m is the arm mass and δ is the distance from the center of mass to the rotation axis. This means that, in order to minimize the coupling between \ddot{z} and the arm tilt, the distance δ needs to be tuned as close as possible to zero.

Several tests have been performed to ascertain the difficulties in setting this distance within the limits of about $10\mu\text{m}$, as required by the Archimedes experiment [17]. The tuning of the center of mass position is done by regulating a set of screws placed on the arm. With the finest screw rotation, the center of mass can be moved by about $1\mu\text{m}$. Tuning operations are performed in air, and tiny mechanical displacements can occur while going into vacuum.

This implies that the tuning accuracy in vacuum is at best around $10\mu\text{m}$, which is still compliant with the requirements. However, in the design of the final balance, the center of mass positioning will be performed by acting remotely on the screws while the system is already in vacuum.

During operation at the Virgo site, the decoupling from translation ground noise has been tested with two methods. The first coarse one was to compare the balance signal with those of nearby seismometers during a far earthquake. In this case, the arrival times of various seismic waves are well separated: The first to occur are the primary waves (P-waves), which are essentially translation pressure waves, hence the secondary waves (S-waves), which are shear waves that can have tilt components depending on their polarization, and finally the surface waves, which have tilt components. While seismometers sense the ground motion, an ideal tiltmeter is expected to be sensitive to surface waves but not to P-waves. The behavior of our tiltmeter during a far earthquake is shown in Fig. 3. As expected, P-waves did not produce a signal above the noise level, while the effect of surface waves has been clearly observed.

A second, more refined method to test the decoupling from \ddot{z} was based on the comparison between tiltmeter and seismometer signals at a frequency where there is mainly translation seismic noise, that is, 0.4 Hz, around the microseismic peak frequency. At this frequency, a seismometer, which is more sensitive to translations than to tilts, would give a signal in which the component due to the ground tilt is negligible, unlike a tiltmeter, which is more sensitive to tilts than to translations. It follows that at 0.4 Hz the coherence between two such signals would be much less than 1, and this is what has been actually observed in our case, where $Coh \approx 0.25$, as shown in Fig. 4. The residual coherence is the consequence of a non-null distance δ . Indeed, if the tiltmeter center of mass does not lie on its rotation axis ($\delta \neq 0$), ground translations give rise to a signal, which is read as a tilt. The *shift-to-tilt* coupling allows an estimate of δ . The coupling, measured as:

$$C = \sqrt{Coh} \frac{\theta}{\ddot{z}/g}$$

results $C \approx 1.2 \times 10^{-3}$, where θ is the balance signal at 0.4 Hz and g is the gravitational acceleration. At first order, the coupling is given by

$$C = \frac{mg \cdot \delta}{I\omega^2}$$

where I and m are the momentum of inertia and the mass of the arm, respectively, and $f = \omega/2\pi$ is the measurement frequency [19]. In the hypothesis that a microseism does not produce ground tilts, the value of the coupling $C = 1.2 \times 10^{-3}$ corresponds to the upper limit $\delta = 15 \times 10^{-6}$ m, consistent with expectations.

2.3 Actuators and control loop

The beam balance is kept at the desired working point through a feedback control system. The loop is closed with electrostatic actuators, as typically used for the control of torsion pendulums [9, 10]. In our case, they are four metallic plates placed along the two sides of the balance arm. This latter is grounded, while the actuators are powered by a DC voltage supplier that can reach the maximum voltage of 2000 V. The actuator torque $\tau = \beta \cdot V^2$ is quadratic in the applied voltage V , with $\beta = 2.5 \times 10^{-11}$ Nm/V². The maximum torque is $\tau_{\max} = 10^{-4}$ Nm. The control signal is linearized by performing the square root of the correction signal before sending it to the actuators. The error signal is provided by the optical

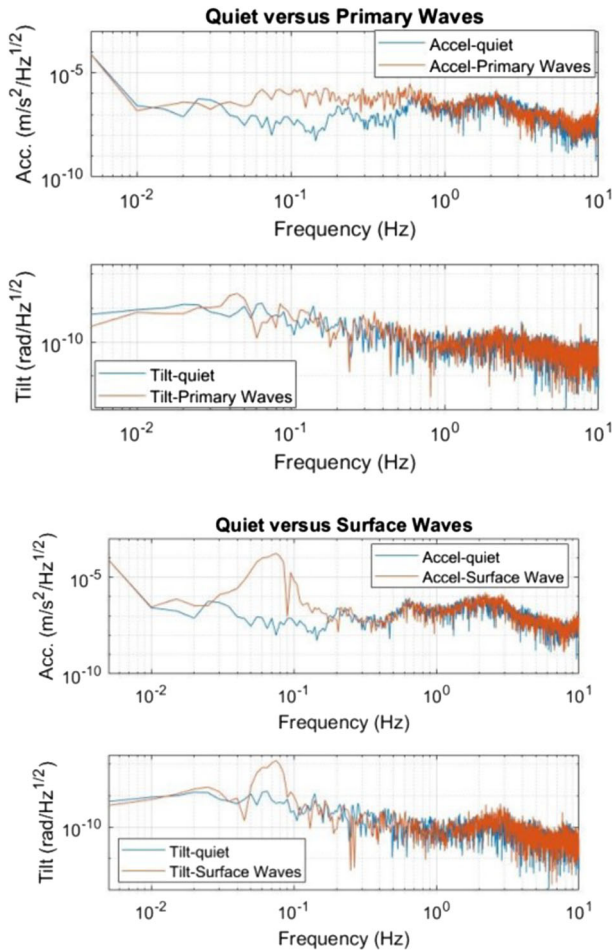


Fig. 3 Earthquake as read by a seismometer and by the tiltmeter. Top figure, upper plots: seismometer signal before (blue) and during (red) the P-waves; Top figure, lower plots: balance signal during the same period. It can be noticed that, during the earthquake, the seismometer senses the higher ground motion while the balance does not, as expected. Bottom figure: the same signals as in Top figure but referring to quiet period (blue) and surface waves. It can be noticed that, as expected, both the seismometer and the tiltmeter sense the higher ground motion

readout, as described in Sect. 2.1. After obtaining a coarse positioning with the optical lever signal, the error signal is switched to the interferometric signal, which provides a finer reference. During the operations at the Virgo site, the error and control signals are acquired and computed by the Virgo processing system [3]. The control loop has unity gain at 0.2 Hz.

3 Results at low frequencies

In the region of tens of mHz, the torque sensitivity reaches the value $\tilde{\tau} \simeq 8 \times 10^{-12} \text{Nm}/\sqrt{\text{Hz}}$. To our knowledge, this result is comparable with or even better than the currently best torque

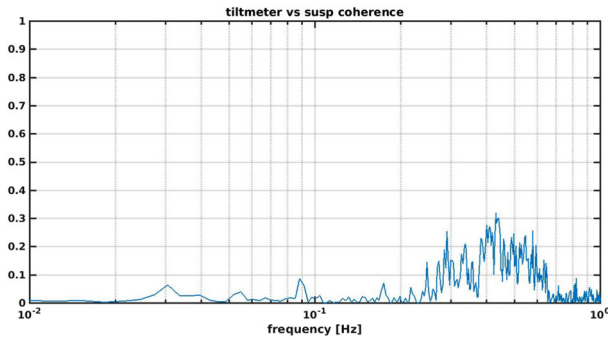


Fig. 4 Coherence of the tiltmeter with a combination of accelerometers at the upper stage of the Virgo superattenuator

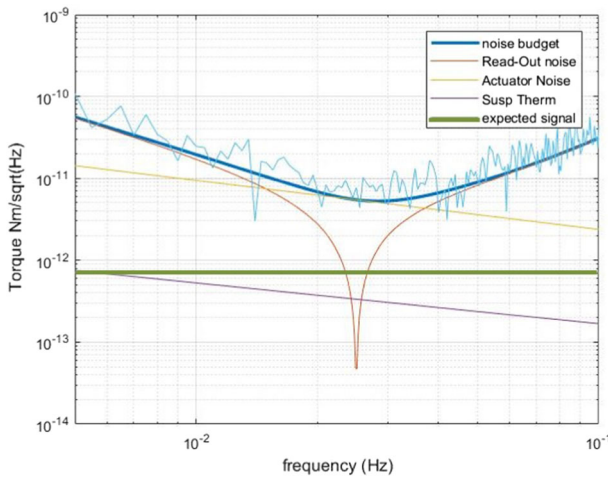


Fig. 5 Sensitivity and noise budget of the balance prototype compared with the expected signal (green line)

sensitivities in the world for balance systems [11]. Actuation and sensing noise are the main limiting noise sources, as reported in Fig. 5. At frequencies below 10 mHz and above 100 mHz, the interferometer signal is indeed coherent with the laser power fluctuations read at the input of the interferometer by an auxiliary photodiode.

In the intermediate region, the major contribution is given by the actuator noise. This can be evaluated considering that presently the actuation is obtained by applying a DC voltage control signal (i.e., not modulated). This implies that the actuation noise \tilde{A}_n , at first order, is proportional to V_{RMS} , the RMS of the control signal: $\tilde{A}_n = \beta \cdot V_{RMS} \tilde{V}_n$, where \tilde{V}_n is the voltage output noise of the amplifier. In the best condition, the balance was operated with tens of volts of static correction, corresponding to the noise reported in Fig. 5.

4 Sensitivity to tilts at high frequencies

Beam balances can be used as rotational sensors. In our case, in the low-frequency region, the sensitivity is not yet sufficiently good to use the balance as tiltmeter to control the Virgo

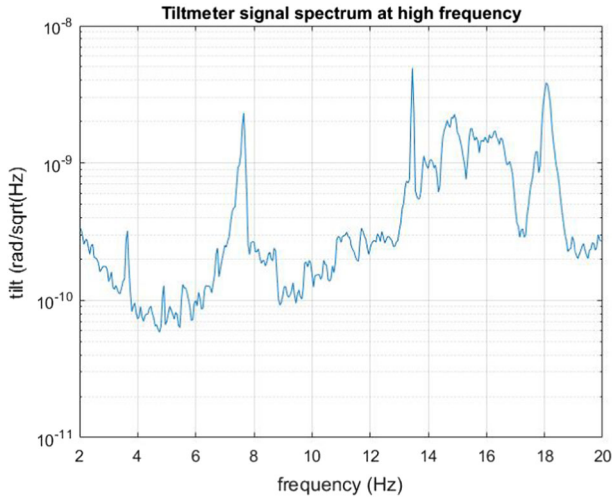


Fig. 6 Spectral density of the tilt amplitude in a quiet night at the Virgo site

interferometer. This is due to the choice of a very light arm, which helps in reaching a very good sensitivity in torque, but makes more difficult its use as a tilt reference. On the contrary, at higher frequencies, far above the resonance frequency, a light arm is not a limitation. Above a few Hz, rotation sensors are expected to be used in future detectors as ground tilt sensors for Newtonian noise subtraction.

The balance has been positioned at the North-end building, on the same floor where other auxiliary systems, like seismometers and other sensors, are located. The balance has been installed just before the start of the Virgo observation run O3 and remained on site for several months. The data taking allowed us to measure the ground tilts and test the coherence with seismometers and with the Virgo interferometer signal.

The results of the tilt measurement are shown in Fig. 6 for the frequency region from 2 to 20 Hz. This interval is particularly interesting for both Virgo and the future Einstein Telescope, whose observation band will extend down to 2 Hz. At a few Hz, the measured tilt reaches $\tilde{\theta} \approx 8 \times 10^{-11} \text{ rad}/\sqrt{\text{Hz}}$. Above 10 Hz, it shows a plateau of a few times $10^{-10} \text{ rad}/\sqrt{\text{Hz}}$ and a series of resonances larger than $10^{-9} \text{ rad}/\sqrt{\text{Hz}}$. The tilt measurement at lower frequencies, around a few Hz, highlights the property of the Virgo site to be quiet in this range.

In the 10–20 Hz interval, the measured tilt is similar to that at the LIGO site [13]. In particular, in the outer ranges (10–13 Hz and 18–20 Hz) the plateau is comparable, whereas in the middle range (between 13 and 18 Hz) the noise is higher. This result is still under investigation. Several resonances are coherent with seismometer signals, corroborating the hypothesis that they are structural resonances of the building. Figure 7 shows the correlation between the tiltmeter and the Virgo interferometer (i.e., gravitational wave) signals. At several frequencies, the tiltmeter is partially coherent with the Virgo interferometer and with seismometers placed in the building. On the other hand, at some frequencies, like 18.65 Hz, the balance signal is coherent with the Virgo interferometer, but not with the seismometers. However, in both cases, estimates of the Newtonian noise coupling is not compatible with a direct Newtonian coupling of ground motion with tilt masses, but rather with, for instance, a coupling mechanism through diffused light.

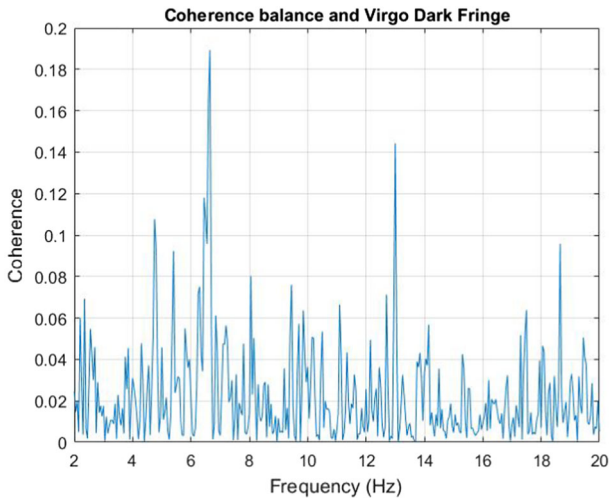


Fig. 7 Coherence of the balance signal with the Virgo interferometer signal

5 Conclusions and next steps

The measurement campaign with the beam balance performed at the Virgo site provided very encouraging results toward the definitive measurement of the weight of electromagnetic vacuum. Indeed, the torque sensitivity at low frequencies reaches the value $8 \times 10^{-12} \text{ Nm}/\sqrt{\text{Hz}}$, which is only a factor ≈ 10 higher than the torque expected in the measurement of vacuum weight.

At present, the sensitivity is limited by the laser amplitude and actuators noises. These can be reduced by stabilizing the laser and using voltage amplifiers with a lower noise. The latter improvement will be possible once the balance will be moved to a more quiet site, such as the SAR-GRAV laboratory, in Sardinia. In these seismic conditions, the force needed to maintain the interferometer locked is expected to be at least an order of magnitude lower; therefore, we could use amplifiers with a lower voltage and hence with a lower noise.

At high frequencies, the balance has shown a very good sensitivity to tilts, allowing us to measure the ground tilt at the Virgo site and to show that at some frequencies the Virgo dark-fringe signal is correlated with the tiltmeter signal. Moving the balance to the SAR-GRAV laboratory will permit a better study of the sensitivity to lower tilts, which will allow a new version of the balance to be used to measure ground tilts in the next Virgo run.

Acknowledgements This work has been partially funded by the PRIN 2017SYRTCN (Progetto di Ricerca Interesse Nazionale—Ministry of University and Research, Italy).

Funding Open access funding provided by Università degli Studi di Napoli Federico II within the CRUI-CARE Agreement.

Data Availability Statement This manuscript has associated data in a data repository. [Authors' comment: This manuscript has associated data in the Virgo Gravitational-Wave detector Data Repository. All data included in this manuscript are available upon request by contacting with the corresponding author.]

Open Access This article is licensed under a Creative Commons Attribution 4.0 International License, which permits use, sharing, adaptation, distribution and reproduction in any medium or format, as long as you give appropriate credit to the original author(s) and the source, provide a link to the Creative Commons licence,

and indicate if changes were made. The images or other third party material in this article are included in the article's Creative Commons licence, unless indicated otherwise in a credit line to the material. If material is not included in the article's Creative Commons licence and your intended use is not permitted by statutory regulation or exceeds the permitted use, you will need to obtain permission directly from the copyright holder. To view a copy of this licence, visit <http://creativecommons.org/licenses/by/4.0/>.

Appendix: The Archimedes and Virgo Collaboration

F. Acernese^{1,2,§}, M. Agathos^{3,§}, L. Aiello^{4,5,§}, A. Ain^{6,7,§}, A. Allocca^{2,8,†,§}, A. Amato^{9,§}, S. Ansoldi^{10,11,§}, S. Antier^{12,§}, M. Arène^{12,§}, N. Arnaud^{13,14,§}, P. Astone^{15,§}, F. Aubin^{16,§}, S. Avino^{2,96,†}, S. Babak^{12,§}, F. Badaracco^{4,5,§}, M. K. M. Bader^{17,§}, S. Bagnasco^{18,§}, J. Baird^{12,§}, G. Ballardin^{14,§}, G. Baltus^{19,§}, C. Barbieri^{20,21,22,§}, P. Barneo^{23,§}, F. Barone^{2,24,§}, M. Barsuglia^{12,§}, D. Barta^{25,§}, A. Basti^{6,7,§}, M. Bawaj^{26,27,§}, M. Bazzan^{28,29,§}, M. Bejger^{30,§}, I. Belahcene^{13,§}, V. Benedetto^{31,§}, S. Bernuzzi^{3,§}, D. Bersanetti^{32,§}, A. Bertolini^{17,§}, M. Bischi^{33,34,§}, M. Bitossi^{6,14,§}, M.-A. Bizouard^{35,§}, F. Bobba^{36,37,§}, M. Boer^{35,§}, G. Bogaert^{35,§}, M. Boldrini^{15,38,§}, F. Bondu^{39,§}, R. Bonnand^{16,§}, B. A. Boom^{17,§}, V. Boschi^{6,§}, V. Boudart^{19,§}, Y. Bouffanaï^{28,29,§}, A. Bozzi^{14,§}, C. Bradaschia^{6,§}, M. Branchesi^{4,5,§}, M. Breschi^{3,§}, T. Briant^{40,§}, A. Brillet^{35,§}, J. Brooks^{14,§}, G. Bruno^{41,§}, T. Bulik^{42,§}, H. J. Bulten^{17,43,§}, D. Buskulic^{16,§}, G. Cagnoli^{9,§}, E. Calloni^{2,8,†,§}, M. Canepa^{32,44,§}, M. Cannavacciuolo^{36,§}, S. Caprara^{15,38,§}, G. Carapella^{36,37,§}, F. Carbognani^{14,§}, M. Carpinelli^{45,46,†,§}, G. Carullo^{6,7,§}, J. Casanueva Diaz^{14,§}, C. Casentini^{47,48,§}, S. Caudill^{17,49,§}, F. Cavalier^{13,§}, R. Cavaliere^{14,§}, G. Cella^{6,§}, P. Cerdá-Durán^{50,§}, E. Cesarini^{48,§}, W. Chaïbi^{35,§}, P. Chanial^{14,§}, E. Chassande-Mottin^{12,§}, F. Chiadini^{37,51,§}, R. Chierici^{52,§}, A. Chincarini^{32,§}, M. L. Chiofalo^{6,7,§}, A. Chiummo^{14,§}, N. Christensen^{35,§}, S. Chua^{40,§}, G. Ciani^{28,29,§}, M. Cieřlar^{30,§}, P. Ciecielag^{30,§}, M. Cifaldi^{47,48,§}, R. Ciolfi^{29,53,§}, F. Cipriano^{35,§}, A. Cirone^{32,44,§}, S. Clesse^{54,§}, F. Cleva^{35,§}, E. Coccia^{4,5,§}, P.-F. Cohadon^{40,§}, D. E. Cohen^{13,§}, M. Colpi^{20,21,§}, L. Conti^{29,§}, I. Cordero-Carrión^{55,§}, S. Corezzi^{26,27,§}, D. Corre^{13,§}, S. Cortese^{14,§}, J.-P. Coulon^{35,§}, M. Croquette^{40,§}, J. R. Cudell^{19,§}, E. Cuoco^{6,14,56,§}, M. Curyło^{42,§}, T. Dal Canton^{13,§}, B. D'Angelo^{32,44,§}, S. D'Antonio^{48,§}, V. Dattilo^{14,§}, M. Davier^{13,§}, M. De Laurentis^{2,8,†,§}, F. De Lillo^{41,§}, F. De Matteis^{47,48,§}, R. De Pietri^{57,58,§}, R. De Rosa^{2,8,§}, C. De Rossi^{14,§}, R. De Simone^{51,§}, J. Degallaix^{59,§}, S. Deléglise^{40,§}, W. Del Pozzo^{6,7,§}, A. Depasse^{41,§}, L. Di Fiore^{2,§}, C. Di Giorgio^{36,37,§}, F. Di Giovanni^{50,§}, T. Di Girolamo^{2,8,§}, A. Di Lieto^{6,7,§}, S. Di Pace^{15,38,§}, I. Di Palma^{15,38,§}, F. Di Renzo^{6,7,§}, T. Dietrich^{17,§}, L. D'Onofrio^{2,8,§}, M. Drago^{4,5,§}, J.-G. Ducoin^{13,§}, O. Durante^{36,37,§}, D. D'Urso^{45,46,†,§}, P.-A. Duverne^{13,§}, M. Eisenmann^{16,§}, L. Errico^{2,8,†,§}, D. Estevez^{60,§}, V. Fafone^{4,47,48,§}, S. Farinon^{32,§}, M. Fays^{19,§}, F. Feng^{12,§}, E. Fenyvesi^{25,61,§}, I. Ferrante^{6,7,§}, F. Fidecaro^{6,7,§}, P. Figura^{42,§}, I. Fiori^{14,§}, R. Fittipaldi^{37,62,§}, V. Fiumara^{37,63,§}, R. Flaminio^{16,64,§}, J. A. Font^{50,65,§}, S. Frasca^{15,38,§}, F. Frasconi^{6,§}, G. G. Fronzé^{18,§}, G. Gagliardi^{2,96,†}, R. Gamba^{3,§}, B. Garaventa^{32,44,§}, F. Garufi^{2,8,§}, G. Gemme^{32,§}, A. Gennai^{6,§}, Archisman Ghosh^{66,§}, B. Giacomazzo^{20,21,22,§}, L. Giacoppo^{15,38,§}, P. Giri^{6,7,§}, F. Gissi^{31,§}, M. Gosselin^{14,§}, R. Gouaty^{16,§}, A. Grado^{2,67,§}, M. Granata^{59,§}, V. Granata^{36,§}, G. Greco^{26,§}, G. Grignani^{26,27,§}, M. Grilli^{15,38,†}, A. Grimaldi^{68,69,§}, S. J. Grimm^{4,5,§}, P. Gruning^{13,§}, G. M. Guidi^{33,34,§}, G. Guixé^{23,§}, Y. Guo^{17,§}, P. Gupta^{17,49,§}, L. Haegel^{12,§}, O. Halim^{11,70,§}, O. Hannuksela^{17,49,§}, T. Harder^{35,§}, K. Haris^{17,49,§}, J. Harms^{4,5,§}, B. Haskell^{30,§}, A. Heidmann^{40,§}, H. Heitmann^{35,§}, P. Hello^{13,§}, G. Hemming^{14,§}, E. Hennes^{17,§}, S. Hild^{17,71,§}, D. Hofman^{59,§}, V. Hui^{16,§}, B. Idzkowski^{42,§}, A. Iess^{47,48,§}, G. Intini^{15,38,§}, T. Jacqmin^{40,§}, K. Janssens^{72,§}, P. Jaranowski^{73,§}, R. J. G. Jonker^{17,§}, F. Kéfélian^{35,§}, C. Karathanasis^{74,§}, S. Katsanevas^{14,§},

I. Khan^{4,48,§}, N. Khetan^{4,5,§}, G. Koekoek^{17,71,§}, S. Koley^{17,§}, M. Kolstein^{74,§}, A. Królak^{75,76,§}, I. La Rosa^{16,§}, D. Laghi^{6,7,§}, A. Lamberts^{35,77,§}, A. Lartaux-Vollard^{13,§}, C. Lazzaro^{28,29,§}, P. Leaci^{15,38,§}, A. Lemaître^{78,§}, N. Leroy^{13,§}, N. Letendre^{16,§}, F. Linde^{17,79,§}, M. Llorens-Monteaudo^{50,§}, A. Longo^{80,81,§}, M. Lorenzini^{47,48,§}, V. Lorient^{82,§}, G. Losurdo^{6,§}, D. Lumaca^{47,48,§}, A. Macquet^{35,§}, C. Magazzù^{6,§}, E. Majorana^{15,38,§}, I. Maksimovic^{82,§}, N. Man^{35,§}, V. Mangano^{15,38,†,§}, M. Mantovani^{14,§}, M. Mapelli^{28,29,§}, F. Marchesoni^{26,83,§}, F. Marion^{16,§}, A. Marquina^{55,§}, S. Marsat^{12,§}, M.A. Marsella^{15,38,†}, F. Martelli^{33,34,§}, M. Martinez^{74,§}, V. Martinez^{9,§}, A. Masserot^{16,§}, S. Mastrogianni^{12,§}, A. Menendez-Vazquez^{74,§}, L. Mereni^{59,§}, M. Merzougui^{35,§}, A. Miani^{68,69,§}, C. Michel^{59,§}, L. Milano^{8,§}, A. Miller^{41,§}, E. Milotti^{11,70,§}, O. Minazzoli^{35,84,§}, Y. Minenkov^{48,§}, L.I. M. Mir^{74,§}, M. Montani^{33,34,§}, F. Morawski^{30,§}, B. Mours^{60,§}, F. Muciaccia^{15,38,§}, R. Musenich^{32,44,§}, A. Nagar^{18,85,§}, I. Nardecchia^{47,48,§}, L. Naticchioni^{15,§}, J. Neilson^{31,37,§}, G. Nelemans^{86,§}, C. Nguyen^{12,§}, S. Nissanke^{17,87,§}, F. Nocera^{14,§}, G. Oganessian^{4,5,§}, C. Olivetto^{14,§}, C. Périgois^{16,§}, G. Pagano^{7,6,§}, G. Pagliaroli^{4,5,§}, C. Palomba^{15,§}, P. T. H. Pang^{17,49,§}, F. Pannarale^{15,38,§}, F. Paoletti^{6,§}, A. Paoli^{14,§}, A. Paolone^{15,88,§}, D. Pascucci^{17,§}, A. Pasqualetti^{14,§}, R. Passaquieti^{6,7,§}, D. Passuello^{6,§}, B. Patricelli^{6,14,§}, M. Pegoraro^{29,§}, G.P. Pepe^{2,8,†}, M. Perciballi^{15,†,§}, A. Perego^{68,69,§}, A. Pereira^{9,§}, A. Perreca^{68,69,§}, S. Perriès^{52,§}, K. S. Phukon^{17,79,§}, O. J. Piccinni^{15,§}, M. Pichot^{35,§}, M. Piendibene^{6,7,§}, F. Piergiorgio^{33,34,§}, L. Pierini^{15,38,§}, V. Pierro^{31,37,§}, G. Pillant^{14,§}, F. Pilo^{6,§}, L. Pinard^{59,§}, I. M. Pinto^{31,37,89,§}, K. Piotrkowski^{41,§}, E. Placidi^{15,38,§}, W. Plastino^{80,81,§}, R. Poggiani^{7,6,§}, E. Polini^{16,§}, P. Popolizio^{14,§}, E. K. Porter^{12,§}, M. Pracchia^{16,§}, T. Pradier^{60,§}, M. Principe^{31,37,89,§}, G. A. Prodi^{69,90,§}, P. Prospero^{47,48,§}, A. Puecher^{17,49,§}, M. Punturo^{26,§}, F. Puosi^{6,7,§}, P. Puppo^{15,†,§}, G. Raaijmakers^{17,87,§}, N. Radulesco^{35,§}, P. Rapagnani^{15,38,†,§}, M. Razzano^{6,7,§}, T. Regimbau^{16,§}, L. Rei^{32,§}, P. Rettegno^{18,91,§}, F. Ricci^{15,38,†,§}, G. Riemenschneider^{18,91,§}, F. Robinet^{13,§}, A. Rocchi^{48,§}, L. Rolland^{16,§}, M. Romanelli^{39,§}, R. Romano^{1,2,§}, A. Romero^{74,§}, L. Rosa^{2,8,†,§}, D. Rosińska^{42,§}, C. Rovelli^{97,98,99,†}, D. Rozza^{45,46,†,§}, P. Ruggi^{14,†,§}, N.L. Saini^{15,38,†}, O. S. Salafia^{20,21,22,§}, L. Salconi^{14,§}, F. Salemi^{68,69,§}, A. Samajdar^{17,49,§}, N. Sanchis-Gual^{92,§}, A. Sanuy^{23,§}, B. Sassolas^{59,§}, O. Sauter^{16,§}, S. Sayah^{59,§}, M. Seglar-Arroyo^{16,§}, D. Sentenac^{14,§}, V. Sequino^{2,8,§}, A. Sharma^{4,5,§}, N. S. Shchepanov^{78,§}, M. Sieniawska^{42,§}, N. Singh^{42,§}, A. Singha^{17,71,§}, V. Sipala^{45,46,†,§}, V. Sordini^{52,§}, F. Sorrentino^{32,§}, N. Sorrentino^{7,6,§}, R. Soulard^{35,§}, V. Spagnuolo^{17,71,§}, M. Spera^{28,29,§}, C. Stachie^{35,§}, D. A. Steer^{12,§}, J. Steinlechner^{17,71,§}, S. Steinlechner^{17,71,§}, D. Stornaiuolo^{2,8,†}, G. Stratta^{93,34,§}, A. Sur^{30,§}, B. L. Swinkels^{17,§}, P. Szczyk^{42,§}, M. Tacca^{17,§}, F. Tafuri^{2,8,†}, A. Tagliacozzo^{2,8,§}, A. J. Tanasijczuk^{41,§}, E. N. Tapia San Martin^{17,§}, M. Tonelli^{6,7,§}, A. Torres-Forné^{50,§}, I. Tosta e Melo^{45,46,†,§}, A. Trapananti^{26,83,§}, F. Travasso^{26,83,§}, M. C. Tringali^{14,§}, L. Troiano^{37,94,§}, A. Trovato^{12,§}, K. W. Tsang^{17,49,95,§}, M. Turconi^{35,§}, A. Utina^{17,71,§}, M. Valentini^{68,69,§}, N. van Bakel^{17,§}, M. van Beuzekom^{17,§}, J. F. J. van den Brand^{17,43,71,§}, C. Van Den Broeck^{17,49,§}, L. van der Schaaf^{17,§}, J. V. van Heijningen^{41,§}, M. Vardaro^{17,79,§}, M. Vasúth^{25,§}, G. Vedovato^{29,§}, D. Verkindt^{16,§}, F. Vetrano^{33,§}, A. Vicere^{33,34,§}, J.-Y. Vinet^{35,§}, H. Vocca^{26,27,§}, R. C. Walet^{17,§}, M. Was^{16,§}, A. Zadrozny^{76,§}, T. Zelenova^{14,§}, J.-P. Zeng²⁹.

¹Dipartimento di Farmacia, Università di Salerno, I-84084 Fisciano, Salerno, Italy ²INFN, Sezione di Napoli, Complesso Universitario di Monte S. Angelo, I-80126 Napoli, Italy ³Theoretisch-Physikalisches Institut, Friedrich-Schiller-Universität Jena, D-07743 Jena, Germany ⁴Gran Sasso Science Institute (GSSI), I-67100 L'Aquila, Italy ⁵INFN, Laboratori Nazionali del Gran Sasso, I-67100 Assergi, Italy ⁶INFN, Sezione di Pisa, I-56127 Pisa, Italy ⁷Università di Pisa, I-56127 Pisa, Italy ⁸Università di Napoli "Federico II," Complesso Universitario di Monte S. Angelo, I-80126 Napoli, Italy ⁹Université de Lyon, Université

Claude Bernard Lyon 1, CNRS, Institut Lumière Matière, F-69622 Villeurbanne, France
¹⁰Dipartimento di Matematica e Informatica, Università di Udine, I-33100 Udine, Italy
¹¹INFN, Sezione di Trieste, I-34127 Trieste, Italy ¹²Université de Paris, CNRS, Astroparticule et Cosmologie, F-75006 Paris, France ¹³Université Paris-Saclay, CNRS/IN2P3, IJCLab, 91405 Orsay, France ¹⁴European Gravitational Observatory (EGO), I-56021 Cascina, Pisa, Italy ¹⁵INFN, Sezione di Roma, I-00185 Roma, Italy ¹⁶Laboratoire d'Annecy de Physique des Particules (LAPP), Univ. Grenoble Alpes, Université Savoie Mont Blanc, CNRS/IN2P3, F-74941 Annecy, France ¹⁷Nikhef, Science Park 105, 1098 XG Amsterdam, the Netherlands
¹⁸INFN Sezione di Torino, I-10125 Torino, Italy ¹⁹Université de Liège, B-4000 Liège, Belgium ²⁰Università degli Studi di Milano-Bicocca, I-20126 Milano, Italy ²¹INFN, Sezione di Milano-Bicocca, I-20126 Milano, Italy ²²INAF, Osservatorio Astronomico di Brera sede di Merate, I-23807 Merate, Lecco, Italy ²³Institut de Ciències del Cosmos, Universitat de Barcelona, C/ Martí i Franquès 1, Barcelona, 08028, Spain ²⁴Dipartimento di Medicina, "Chirurgia e Odontoiatria Scuola Medica Salernitana," Università di Salerno, I-84081 Baronissi, Salerno, Italy ²⁵Wigner RCP, RMKI, H-1121 Budapest, Konkoly Thege Miklós út 29-33, Hungary ²⁶INFN, Sezione di Perugia, I-06123 Perugia, Italy ²⁷Università di Perugia, I-06123 Perugia, Italy ²⁸Università di Padova, Dipartimento di Fisica e Astronomia, I-35131 Padova, Italy ²⁹INFN, Sezione di Padova, I-35131 Padova, Italy ³⁰Nicolaus Copernicus Astronomical Center, Polish Academy of Sciences, 00-716, Warsaw, Poland ³¹Dipartimento di Ingegneria, Università del Sannio, I-82100 Benevento, Italy ³²INFN, Sezione di Genova, I-16146 Genova, Italy ³³Università degli Studi di Urbino "Carlo Bo," I-61029 Urbino, Italy ³⁴INFN, Sezione di Firenze, I-50019 Sesto Fiorentino, Firenze, Italy ³⁵Artemis, Université Côte d'Azur, Observatoire Côte d'Azur, CNRS, F-06304 Nice, France ³⁶Dipartimento di Fisica "E.R. Caianiello," Università di Salerno, I-84084 Fisciano, Salerno, Italy ³⁷INFN, Sezione di Napoli, Gruppo Collegato di Salerno, Complesso Universitario di Monte S. Angelo, I-80126 Napoli, Italy ³⁸Università di Roma "La Sapienza," I-00185 Roma, Italy ³⁹Univ Rennes, CNRS, Institut FOTON - UMR6082, F-3500 Rennes, France ⁴⁰Laboratoire Kastler Brossel, Sorbonne Université, CNRS, ENS-Université PSL, Collège de France, F-75005 Paris, France ⁴¹Université catholique de Louvain, B-1348 Louvain-la-Neuve, Belgium
⁴²Astronomical Observatory Warsaw University, 00-478 Warsaw, Poland ⁴³VU University Amsterdam, 1081 HV Amsterdam, the Netherlands ⁴⁴Dipartimento di Fisica, Università degli Studi di Genova, I-16146 Genova, Italy ⁴⁵Università degli Studi di Sassari, I-07100 Sassari, Italy ⁴⁶INFN, Laboratori Nazionali del Sud, I-95125 Catania, Italy ⁴⁷Università di Roma Tor Vergata, I-00133 Roma, Italy ⁴⁸INFN, Sezione di Roma Tor Vergata, I-00133 Roma, Italy ⁴⁹Institute for Gravitational and Subatomic Physics (GRASP), Utrecht University, Princetonplein 1, 3584 CC Utrecht, the Netherlands ⁵⁰Departamento de Astronomía y Astrofísica, Universitat de València, E-46100 Burjassot, València, Spain ⁵¹Dipartimento di Ingegneria Industriale (DIIN), Università di Salerno, I-84084 Fisciano, Salerno, Italy
⁵²Institut de Physique des 2 Infinis de Lyon (IP2I), CNRS/IN2P3, Université de Lyon, Université Claude Bernard Lyon 1, F-69622 Villeurbanne, France ⁵³INAF, Osservatorio Astronomico di Padova, I-35122 Padova, Italy ⁵⁴Université libre de Bruxelles, Avenue Franklin Roosevelt 50 - 1050 Bruxelles, Belgium ⁵⁵Departamento de Matemáticas, Universitat de València, E-46100 Burjassot, València, Spain ⁵⁶Scuola Normale Superiore, Piazza dei Cavalieri, 7 - 56126 Pisa, Italy ⁵⁷Dipartimento di Scienze Matematiche, Fisiche e Informatiche, Università di Parma, I-43124 Parma, Italy ⁵⁸INFN, Sezione di Milano Bicocca, Gruppo Collegato di Parma, I-43124 Parma, Italy ⁵⁹Laboratoire des Matériaux Avancés (LMA), Institut de Physique des 2 Infinis (IP2I) de Lyon, CNRS/IN2P3, Université de Lyon, Université Claude Bernard Lyon 1, F-69622 Villeurbanne, France ⁶⁰Université de Strasbourg, CNRS, IPHC UMR 7178, F-67000 Strasbourg, France ⁶¹Institute for Nuclear Research,

Hungarian Academy of Sciences, Bem t'er 18/c, H-4026 Debrecen, Hungary ⁶²CNR-SPIN, c/o Università di Salerno, I-84084 Fisciano, Salerno, Italy ⁶³Scuola di Ingegneria, Università della Basilicata, I-85100 Potenza, Italy ⁶⁴gravitational wave Science Project, National Astronomical Observatory of Japan (NAOJ), Mitaka City, Tokyo 181-8588, Japan ⁶⁵Observatori Astronòmic, Universitat de València, E-46980 Paterna, València, Spain ⁶⁶Universiteit Gent, B-9000 Gent, Belgium ⁶⁷INAF, Osservatorio Astronomico di Capodimonte, I-80131 Napoli, Italy ⁶⁸Università di Trento, Dipartimento di Fisica, I-38123 Povo, Trento, Italy ⁶⁹INFN, Trento Institute for Fundamental Physics and Applications, I-38123 Povo, Trento, Italy ⁷⁰Dipartimento di Fisica, Università di Trieste, I-34127 Trieste, Italy ⁷¹Maastricht University, P.O. Box 616, 6200 MD Maastricht, the Netherlands ⁷²Universiteit Antwerpen, Prinsstraat 13, 2000 Antwerpen, Belgium ⁷³University of Białystok, 15-424 Białystok, Poland ⁷⁴Institut de Física d'Altes Energies (IFAE), Barcelona Institute of Science and Technology, and ICREA, E-08193 Barcelona, Spain ⁷⁵Institute of Mathematics, Polish Academy of Sciences, 00656 Warsaw, Poland ⁷⁶National Center for Nuclear Research, 05-400 Świerk-Otwock, Poland ⁷⁷Laboratoire Lagrange, Université Côte d'Azur, Observatoire Côte d'Azur, CNRS, F-06304 Nice, France ⁷⁸NAVIER, École des Ponts, Univ Gustave Eiffel, CNRS, Marne-la-Vallée, France ⁷⁹Institute for High-Energy Physics, University of Amsterdam, Science Park 904, 1098 XH Amsterdam, the Netherlands ⁸⁰Dipartimento di Matematica e Fisica, Università degli Studi Roma Tre, I-00146 Roma, Italy ⁸¹INFN, Sezione di Roma Tre, I-00146 Roma, Italy ⁸²ESPCI, CNRS, F-75005 Paris, France ⁸³Università di Camerino, Dipartimento di Fisica, I-62032 Camerino, Italy ⁸⁴Centre Scientifique de Monaco, 8 quai Antoine 1er, MC-98000, Monaco ⁸⁵Institut des Hautes Etudes Scientifiques, F-91440 Bures-sur-Yvette, France ⁸⁶Department of Astrophysics/IMAPP, Radboud University Nijmegen, P.O. Box 9010, 6500 GL Nijmegen, the Netherlands ⁸⁷GRAPPA, Anton Pannekoek Institute for Astronomy and Institute for High-Energy Physics, University of Amsterdam, Science Park 904, 1098 XH Amsterdam, the Netherlands ⁸⁸Consiglio Nazionale delle Ricerche - Istituto dei Sistemi Complessi, Piazzale Aldo Moro 5, I-00185 Roma, Italy ⁸⁹Museo Storico della Fisica e Centro Studi e Ricerche "Enrico Fermi," I-00184 Roma, Italy ⁹⁰Università di Trento, Dipartimento di Matematica, I-38123 Povo, Trento, Italy ⁹¹Dipartimento di Fisica, Università degli Studi di Torino, I-10125 Torino, Italy ⁹²Centro de Astrofísica e Gravitação (CENTRA), Departamento de Física, Instituto Superior Técnico, Universidade de Lisboa, 1049-001 Lisboa, Portugal ⁹³INAF, Osservatorio di Astrofisica e Scienza dello Spazio, I-40129 Bologna, Italy ⁹⁴Dipartimento di Scienze Aziendali - Management and Innovation Systems (DISA-MIS), Università di Salerno, I-84084 Fisciano, Salerno, Italy ⁹⁵Van Swinderen Institute for Particle Physics and Gravity, University of Groningen, Nijenborgh 4, 9747 AG Groningen, the Netherlands ⁹⁶Consiglio Nazionale delle Ricerche, Istituto Nazionale di Ottica (INO), via Campi Flegrei 34-Comprensorio A. Olivetti, 80078 Pozzuoli (Na), Italy ⁹⁷Centre de Physique Théorique Campus of Luminy, Case 907, F-13288 Marseille, France ⁹⁸Aix-Marseille Université Site du Pharo - 58 bd Charles Livon - F-13284 Marseille, France ⁹⁹Université de Toulon, Campus de La Garde - La Valette Avenue de l'Université F-83130 LA GARDE Toulon, France.

References

1. B.P. Abbott et al., LIGO-Virgo collaboration: "Observation of gravitational waves from a Binary Black Hole Merger". *Phys. Rev. Lett.* **116**(6), 061102 (2016)

2. B.P. Abbott et al., LIGO-Virgo collaboration: “GWTC-1: a gravitational-wave transient catalog of compact binary mergers observed by LIGO and Virgo during the first and second observing runs”. *Phys. Rev. X* **9**(3), 031040 (2019)
3. F. Acernese et al., Virgo Coll: “Advanced Virgo: a second-generation interferometric gravitational wave detector”. *Class. Quantum Gravit.* **32**(2), 024001 (2015)
4. J. Aasi et al., LIGO Scientific Collaboration: “Advanced LIGO”. *Class. Quantum Gravit.* **32**, 074001 (2015)
5. T. Akutsu, KAGRA collaboration: “KAGRA: 2.5 Generation Interferometric gravitational wave Detector”. *Nat. Astron.* **3**(1), 35–40 (2019)
6. K.L. Dooley, J.R. Leong et al., GEO 600 and the GEO-HF upgrade program: successes and challenges. *Class. Quantum Gravit.* **33**, 075009 (2016)
7. N. Bartolo, C. Caprini et al., Science with the space-based interferometer LISA. IV: Probing inflation with gravitational waves. *JCAP* **12**, 026 (2016)
8. L. Zhu, Q. Liu et al., Test of the equivalence principle with chiral masses using a rotating torsion pendulum. *Phys. Rev. Lett.* **121**(26), 261101 (2018)
9. G. Russano, A. Cavalleri et al., Measuring fN force variations in the presence of constant nN forces: a torsion pendulum ground test of the LISA Pathfinder free-fall mode. *Class. Quantum Gravit.* **35**(3), 035017 (2018)
10. M. Bassan, M. De Laurentis et al., Improving sensitivity and duty-cycle of a double torsion pendulum. *Class. Quantum Gravit.* **36**(12), 125004 (2019)
11. K. Venkateswara, C.A. Hagedorn et al., A high-precision mechanical absolute-rotation sensor. *Rev. Sci. Instrum.* **85**, 015005 (2014)
12. P. Ross, K. Venkateswara et al., Towards windproofing LIGO: Reducing the effect of wind-driven floor tilt by using rotation sensors inactive seismic isolation” e-Print: 2003.06447
13. M. Coughlin, J. Harms et al., Implications of dedicated seismometer measurements on Newtonian-noise cancellation for Advanced LIGO. *Phys. Rev. Lett.* **121**(22), 221104 (2018)
14. F. Badaracco, J. Harms, Optimization of seismometer arrays for the cancellation of Newtonian noise from seismic body waves. *Class. Quantum Gravit.* **36**(14), 145006 (2019)
15. J. Harms, K. Venkateswara, Newtonian-noise cancellation in large-scale interferometric GW detectors using seismic tiltmeters. *Class. Quantum Gravit.* **33**(23), 234001 (2016)
16. G. Bimonte, E. Calloni, G. Esposito, L. Rosa, Energy-momentum tensor for a Casimir apparatus in a weak gravitational field. *Phys. Rev. D* **74**, 085011 (2006)
17. E. Calloni, M. De Laurentis, R. De Rosa, L. Di Fiore, G. Esposito, F. Garufi, L. Rosa, C. Rovelli, P. Ruggi, F. Tafuri et al., Towards weighing the condensation energy to ascertain the Archimedes force of vacuum. *Phys. Rev. D* **90**, 022002 (2014)
18. S. Avino, E. Calloni et al., Progress in a vacuum weight search experiment. *MDPI Phys.* **2**(1), 1–13 (2020)
19. C.C. Speake, D.B. Newell, The design and application of a novel high frequency tiltmeter. *Rev. Sci. Instrum.* **61**, 1500 (1990)
20. F. Matichard, M. Evans, Review: tilt-free low-noise seismometry. *Bull. Seismol. Soc. Am.* **105**(2A), 497–510 (2015)